Available online at www.sciencedirect.com
ScienceDirect
Journal of the European Ceramic Society 27 (2007) 2849–2853
www.elsevier.com/locate/jeurceramsoc

Microstructure and dielectric properties of amorphous $BaSm_2Ti_4O_{12}$ thin films for MIM capacitor

Young Hun Jeong [a], Jong Bong Lim [a], Jae Chul Kim [a], Sahn Nahm [a,*], Ho-Jung Sun [b], Hwack Joo Lee [c]

[a] *Department of Materials Science and Engineering, Korea University, 1-5 Ka, Anam-Dong, Sungbuk-Ku, Seoul 136-701, Republic of Korea*
[b] *Department of Materials Science and Engineering, Kunsan National University, San 68, Miryong-dong, Gunsan, Jeonbuk 573-701, Republic of Korea*
[c] *New Materials Evaluation Center, Korea Research Institute of Standards and Science, Daeduk Science Town, Taejon 305-600, Republic of Korea*

Available online 12 December 2006

Abstract

$BaSm_2Ti_4O_{12}$ (BST) film grown at room temperature was amorphous, while the film grown at 300 °C was also amorphous but contained a small amount of crystalline $Sm_2Ti_2O_7$ (ST). The crystalline BST phase was formed when the film was grown at 700 °C and subjected to rapid thermal annealing (RTA) at 900 °C. On the other hand, the ST phase was formed in the film grown at 300 °C and subjected to RTA at 900 °C. A high capacitance density of 2.12 fF/μm^2 and a low leakage current density of 1.15 fA/pF V were obtained from the 150 nm-thick BST film grown at 300 °C. Its capacitance density could conceivably be further increased by decreasing the thickness of the film. It had linear and quadratic coefficients of capacitance of −785 ppm/V and 5.8 ppm/V^2 at 100 kHz, respectively. Its temperature coefficient of capacitance was also low, being approximately 255 ppm/°C at 100 kHz.

Keywords: Films; Electrical properties; $BaSm_2Ti_4O_{12}$; Capacitors

1. Introduction

Metal–insulator–metal (MIM) capacitors have been widely investigated for their use in passive device for radio-frequency (RF) and the analog/mixed-signal integrated circuits for wireless communication. To minimize the chip size and cost of integrated circuits (IC), it is natural that MIM capacitors should be down-scaled.[1] Therefore, high k dielectric materials have attracted much attention because they can afford a high capacitance density for the same capacitor size. According to the International Technology Roadmap for Semiconductor (ITRS), a high capacitance density will be required for analog capacitors (10 fF/μm^2) and RF bypass capacitors (30 fF/μm^2) by the years 2016 and 2010, respectively.[1] In previous studies, the conventional silicon oxide and silicon nitride, which have low k values of 3–7 were replaced by dielectric materials with a high k value of around 20–30, such as HfO_2 and Ta_2O_5.[2–7] A MIM capacitor made using a film with an Al_2O_3 and HfO_2 laminate structure was also investigated to obtain better electrical performance than that of the films grown using pure dielectric materials such as HfO_2 and Al_2O_3.[8,9] However, they could not satisfy all the requirements for MIM capacitors simultaneously, which are a high capacitance density, voltage linearity of the capacitance, temperature stability, and a low leakage current.[1,10] Recently, it was reported that a 17 nm-thick TiTaO film had a very high capacitance density of 23 fF/μm, which would satisfy the requirement for RF MIM capacitors, however its leakage current density was relatively high.[11] A high capacitance density of 17.6 fF/μm^2 was also obtained from a capacitor consisting of a 8 nm-thick Nb_2O_5 film with HfO_2 (3 nm)/Al_2O_3 (1 nm) barriers.[12] However, the problem of its comparatively low leakage current density remains to be overcome.

Microwave dielectric materials are well known for their high k value, high quality factor (Q-factor) and good temperature stability and, thus, they can be used as MIM capacitors.[13] Especially, $BaSm_2Ti_4O_{12}$ (BST) ceramics show good microwave dielectric properties with values of $Q = 2289$ at 3.6 GHz and $k = 78.91$, along with good temperature stability of the resonance frequency.[14] Crystalline BST thin film was also shown to be potentially applicable to MIM capacitors.[15] However, the process temperature used to grow crystalline BST films is higher than that used for the VLSI back-end process (≤400 °C).

* Corresponding author. Tel.: +82 2 3290 3279; fax: +82 2 928 3584.
E-mail address: snahm@korea.ac.kr (S. Nahm).

0955-2219/$ – see front matter © 2006 Elsevier Ltd. All rights reserved.
doi:10.1016/j.jeurceramsoc.2006.11.001

Consequently, it is necessary to lower the process temperature used for fabrication of the device within the thermal budget of back-end process. In this study, amorphous BST films were grown at room temperature and 300 °C and their dielectric properties were investigated in order to assess their potential for use in MIM capacitors.

2. Experimental procedure

Amorphous $BaSm_2Ti_4O_{12}$ films were grown on Pt/Ti/SiO_2/Si(1 0 0) substrate by RF-magnetron sputtering using a 3 in.-diameter BST target, which was synthesized by the conventional solid state method. Deposition was carried out between room temperature and 700 °C in an oxygen and argon (O_2:Ar = 1:4) atmosphere at a total pressure of 8 mTorr, sputtering power of 120 W and deposition time of 3 h. The structure of the film was studied using X-ray diffraction (XRD; Rigaku D/max-RC, Japan). To measure the dielectric properties at low frequencies (100 kHz to 1 MHz), Pt was deposited on the BST thin films as the top electrode of MIM capacitors using conventional dc sputtering. The top electrode was patterned using a shadow mask to form a disk with diameter of 360 μm. The capacitance and dissipation factor were measured by precision LCR meter (Agilent 4285A, USA). Leakage current was measured using Source meter (Keithley2400, USA).

3. Results and discussion

Fig. 1 shows the XRD patterns of the BST films grown at various temperatures. An amorphous phase was formed in the film grown at room temperature. Moreover, for the films grown at high temperatures, no peaks were observed for the crystalline phase. Therefore, it is considered that these films also have an amorphous phase. However, it is also possible that the crystalline phase was formed in these films but its amount is too small to be detected in the XRD patterns.

Fig. 2 also shows the XRD patterns of the films grown at various temperatures and subjected to RTA at 900 °C for 3 min. For

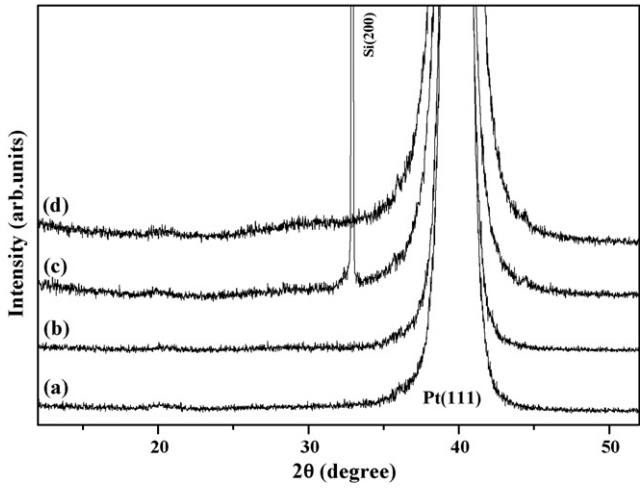

Fig. 1. X-ray diffraction patterns of the films grown at: (a) room temperature; (b) 300 °C; (c) 600 °C; (d) 700 °C.

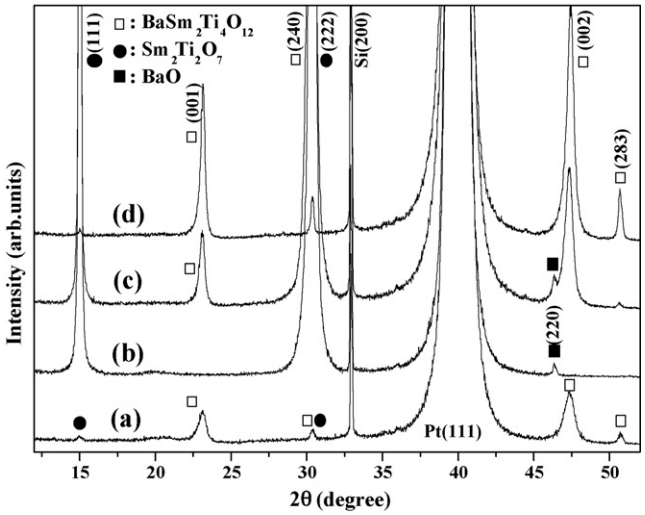

Fig. 2. X-ray diffraction patterns of the films grown at: (a) room temperature; (b) 300 °C; (c) 600 °C; (d) 700 °C and subjected to rapid thermal annealing at 900 °C.

the film deposited at room temperature and annealed at 900 °C, a crystalline BST phase was found and a small amount of ST phase was also observed, as shown in Fig. 2(a). However, only peaks for the ST phase were found in the film grown at 300 °C and annealed at 900 °C. The intensity of the [1 1 1] peak is very large, indicating that the ST film has its preferred orientation along the [1 1 1] direction. A small peak for BaO phase was also observed in this film [see Fig. 2(b)]. When the growth temperature exceeded 300 °C, BST phase started to be form and both ST and BST phases coexisted in these films, as shown in Fig. 2(c). Furthermore, for the film grown at 700 °C and annealed at 900 °C, only crystalline BST film was formed, as shown in Fig. 2(d). According to previous works, ST ceramic is formed when the sintering temperature of the specimen with the nominal composition of BST is lower than 1150 °C.[16] On the other hand, when the sintering temperature of the specimen exceeds 1150 °C, BST ceramic is formed.[17] Therefore, ST phase is considered to be a low temperature phase of BST ceramics, which is formed when the sintering temperature is not high enough to sinter the BST phase. These results can be used to explain the phase changes, which occurred in the BST films with respect to the growth temperature.

When it was deposited at room temperature, the BST film was amorphous and crystalline BST phase was formed from the amorphous phase during the annealing process at 900 °C, resulting in the formation of the BST crystalline film shown in Fig. 2(a). On the other hand, when the film was grown at 300 °C, although they were not detected in XRD patterns, small ST crystals could be formed instead of BST crystals because the growth temperature was too low for BST crystal to be formed. When this film was annealed at 900 °C, these small ST crystals, which were formed during the deposition at 300 °C, grew and developed to produce the ST crystalline film shown in Fig. 2(b). As the growth temperature was increased, small BST crystals started to form and both small ST and BST crystals coexisted in the film. These small crystals grew during the

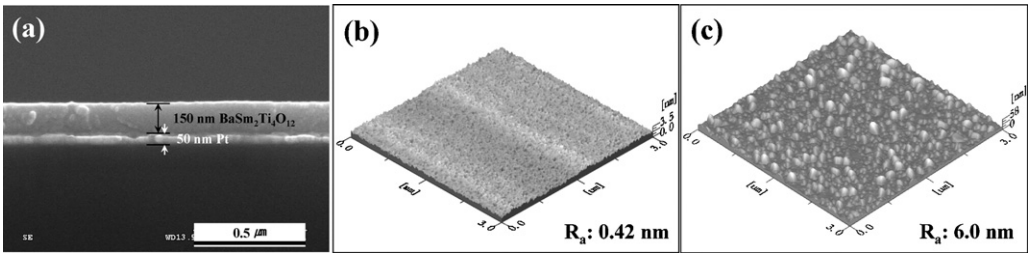

Fig. 3. (a) SEM and (b) AFM images of the film grown at 300 °C and (c) AFM image of the film grown at room temperature.

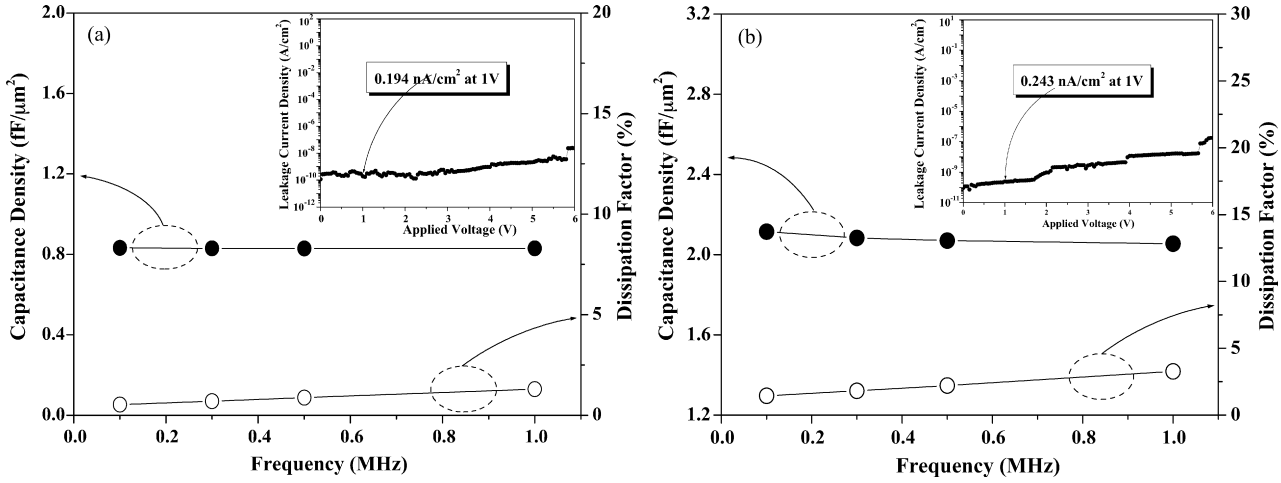

Fig. 4. Capacitance densities and dissipation factors of (a) the 175 nm-thick amorphous BST film grown at room temperature and (b) the 150 nm-thick BST film grown at 300 °C measured at various frequencies. Each inset shows the leakage current density of the films as a function of the applied voltage.

annealing process at 900 °C resulting in the formation of a film containing both crystalline ST and BST phases [see Fig. 2(c)]. Furthermore, when the growth temperature exceeded 600 °C, only small BST crystals were formed during the deposition and these crystals grew during the process of annealing at 900 °C forming the film with BST crystalline phase shown in Fig. 2(d).

Fig. 3(a) shows a SEM image of the BST film grown at 300 °C. The BST film was well developed and the interface between the BST film and Pt electrode is relatively sharp. A similar result was also observed for the BST film grown at room temperature. The surface morphology of the BST films was also studied using AFM, as shown in Fig. 3(b) and (c). The BST film grown at 300 °C showed a very smooth surface with an average roughness of 0.42 nm, as shown in Fig. 3(b). For the film grown at room temperature, although the surface roughness was increased, it also had a relatively smooth surface [see Fig. 3(c)]. Therefore, it is considered that the BST films were well developed on the $Pt/Ti/SiO_2/Si(1\,0\,0)$ substrate.

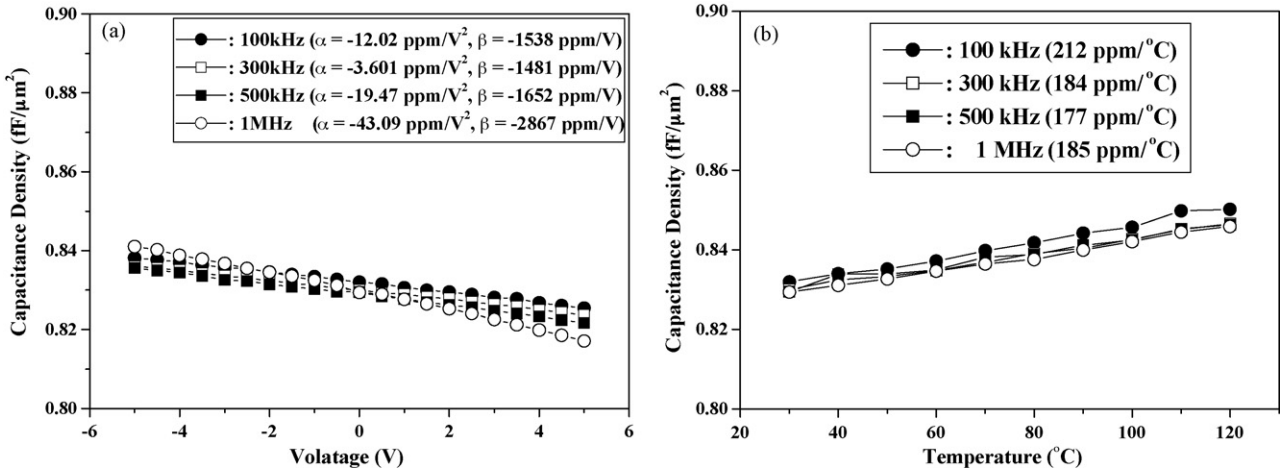

Fig. 5. Variation in the capacitance density with (a) applied voltage and (b) temperature at various frequencies for the 175 nm-thick amorphous BST film grown at room temperature.

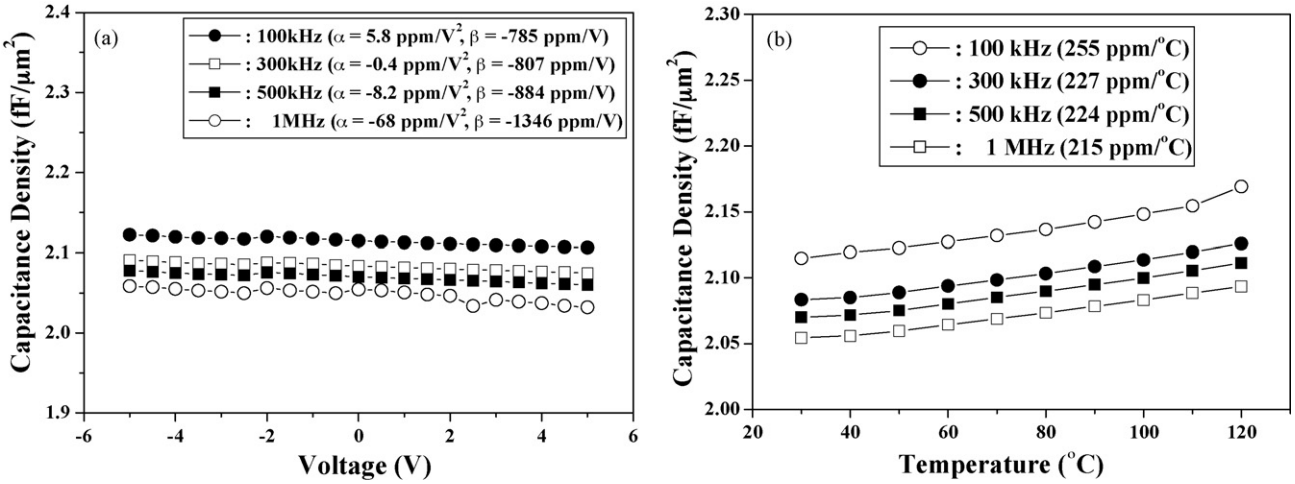

Fig. 6. Variation in the capacitance density with (a) applied voltage and (b) temperature at various frequencies for the 150 nm-thick BST film grown at 300 °C.

Fig. 4(a) shows the capacitance density and dissipation factor of the175 nm-thick amorphous BST film grown at room temperature measured at various frequencies. The capacitance density of the BST film was low, being approximately 0.832 fF/μm^2 and its frequency dependence was negligible. The effective k value of the amorphous BST film was approximately 16.5. According to the ITRS, a capacitance density of 4.0 fF/μm^2 is required for precision analog capacitors. Thus, the capacitance density of the 175 nm-thick amorphous BST film is too low for it to be used as a MIM capacitor. However, since its thickness was 175 nm, its capacitance density could be increased by decreasing the thickness of the film. The dissipation factor of the amorphous BST film was 0.0053 at 100 kHz and increased with increasing frequency, reaching 0.015 at 1.0 MHz. The variation of the leakage current density is also illustrated in the inset of Fig. 4(a). The leakage current density of the BST film was 0.194 nA/cm^2 at 1 V. According to the ITRS, a leakage current density of 7 fA/pF V or lower is required for precision analog capacitors.[1] The leakage current density of the BST film was approximately 2.33 fA/pF V and, therefore, satisfied the required ITRS requirement.

The capacitance density and dissipation factor of the 150 nm-thick BST film grown at 300 °C were also measured as a function of the frequency, as shown in Fig. 4(b). The capacitance density was 2.12 fF/μm^2 and it slightly decreased with increasing frequency but this variation was not significant. The effective k value of this film was high, being approximately 45. The effective k value of the ST ceramics was 61. This shows that it has a high capacitance density and a high k value compared with those of the amorphous film grown at room temperature. Therefore, this result also implies that small crystalline ST phases are formed in this film. Even though its capacitance density is low, it could conceivably be increased by decreasing the thickness of the film. The dissipation factor of this film increased from 0.007 to 0.035 as the frequency increased from 100 kHz to 1.0 MHz. The inset shows the leakage current density of this film as a function of the applied voltage. Its leakage current density was very low, being approximately 1.15 fA/pF V, and satisfied the ITRS requirement.

The linearity of the variation in the capacitance with applied voltage or temperature is very important parameter for MIM capacitors. The voltage coefficients of capacitance (VCC) of the BST films can be obtained from the capacitance and voltage measurements using the second order polynomial equation, $C(V)/C_0 = \alpha (V)^2 + \beta (V) + 1$, where C_0 is the zero-biased capacitance, and α and β represent the quadratic and linear VCCs, respectively.[3] Fig. 5(a) shows the variation in the capacitance density with the applied voltage at various frequencies for the amorphous BST film grown at room temperature. The frequency dependence of the VCC was not significant. For the film measured at 100 kHz, the values of α and β were -12.02 ppm/V^2 and -1538 ppm/V, respectively. The quadratic VCC is slightly lower, whereas the linear VCC is larger, than the value required ($\alpha < 100$ ppm/V^2, $\beta < 1000$ ppm/V) for precision analog capacitors. The temperature coefficient of capacitance (TCC) was also measured from 25 to 120 °C at various frequencies as shown in Fig. 5(b). As the temperature increased, the capacitance density increased indicating that the amorphous BST film has a positive TCC. The TCC of the amorphous BST film measured at 100 kHz was 212 ppm/°C. Therefore, the amorphous BST film has good temperature stability.

The VCC of the BST film grown at 300 °C was also obtained from the capacitance and voltage measurements as shown in Fig. 6(a). The values of α and β measured at 100 kHz were about 5.8 ppm/V^2 and -785 ppm/V, respectively. These values satisfied the requirement for precision analog capacitors. The TCC of this film was also measured from the variation in the capacitance with the temperature, as shown in Fig. 6(b). The TCC of this film measured at 100 kHz was 255 ppm/°C and, thus, the BST film grown at 300 °C has good temperature stability.

4. Conclusions

The BST film grown at room temperature is amorphous but the film grown at 300 °C contains a small amount of crystalline ST. The 175 nm-thick amorphous BST film grown at room temperature had a capacitance density of 0.832 fF/μm^2 and a low leakage current density of 2.33 fA/pF V. The VCCs and TCC of

the amorphous BST films were also good. A capacitance density of 2.12 fF/μm^2 was obtained for the 150 nm-thick BST film grown at 300 °C, which could conceivably be further increased by decreasing the thickness of the film. This BST film was found to have a very low leakage current density, good temperature stability, and a satisfactory quadratic VCC. Therefore, BST film grown at 300 °C is a good candidate material for MIM capacitors.

Acknowledgments

This work was supported by the Ministry of Commerce, Industry and Energy through the Standardization project and one of the authors also acknowledges that this work was financially supported by the Ministry of Science and Technology through the NRL project.

References

1. *The International Technology Roadmap for Semiconductors*, Semiconductor Industry Association, San Jose, CA, 2004.
2. Kim, S. J., Cho, B. J., Li, M. F., Zhu, A., Chin, A. and Kwong, D.-L., HfO_2 and lanthanide-doped HfO_2 MIM capacitors for RF/mixed IC applications. *VLSI Symp. Tech. Dig.*, 2003, 77–78.
3. Hu, H., Zhu, C., Lu, Y. F., Li, M. F., Cho, B. J. and Choi, W. K., A high performance MIM capacitor using HfO_2 dielectrics. *IEEE Electr. Dev. Lett.*, 2002, **23**, 514–516.
4. Kim, S. J., Cho, B. J., Ding, S. J., Li, M.-F., Yu, M. B., Zhu, C. *et al.*, Engineering of voltage nonlinearity in high-*k* MIM capacitor for analog/mixed-signal ICs. *Symp. VLSI Tech. Dig.*, 2004, 218–219.
5. Ishikawa, T., Kodama, D., Matsui, Y., Hiratani, M., Furusawa, T. and Hisamoto, D., High-capacitance Cu/Ta_2O_5/Cu MIM structure for SoC applications featuring a single-mask add-on process. *IEDM Tech. Dig.*, 2002, 940–942.
6. Yang, M. Y., Huang, C. H., Chin, A., Zhu, C., Cho, B. J., Li, M. F. *et al.*, Very high density RF MIM capacitors (17 fF/μm^2) using high-*k* Al_2O_3 doped Ta_2O_5 dielectrics. *IEEE Microw. Wireless Comp. Lett.*, 2003, **13**, 431–433.
7. Perng, T.-H., Chien, C.-H., Chen, C.-W., Lehnen, P. and Chang, C.-Y., High-density MIM capacitors with HfO_2 dielectrics. *Thin Solid Films*, 2004, **469/470**, 345–349.
8. Hu, H., Ding, S.-J., Lim, H. F., Zhu, C., Li, M. F., Kim, S. J. *et al.*, High performance ALD HfO_2–Al_2O_3 laminate MIM capacitors for RF and mixed signal IC application. *IEDM Tech. Dig.*, 2003, 379–382.
9. Ding, S.-J., Hu, H., Zhu, C., Li, M. F., Kim, S. J., Cho, B. J. *et al.*, Evidence and understanding of ALD HfO_2–Al_2O_3 laminate MIM capacitors outperforming sandwich counterparts. *IEEE Electr. Dev. Lett.*, 2004, **25**, 681–683.
10. Wenger, C., Darbrowski, J., Zaumseil, P., Sorge, R., Formanek, P., Lippert, G. *et al.*, First investigation of metal–insulator–metal (MIM) capacitor using Pr_2O_3 dielectrics. *Mat. Sci. Semicon. Proc.*, 2004, **7**, 227–230.
11. Chiang, K. C., Lai, C. H., Chin, A., Wang, T. J., Chiu, H. F., Chen, J.-R. *et al.*, Very high-density (23 fF) RF MIM capacitors using high-*k* TaTiO as the dielectric. *IEEE Electr. Dev. Lett.*, 2005, **26**, 728–730.
12. Kim, S. J., Cho, B. J., Yu, M. B., Li, M.-F., Xiong, Y.-Z., Zhu, C. *et al.*, Metal–insulator–metal RF bypass capacitor using niobium oxide (Nb_2O_5) with HfO_2/Al_2O_3 barriers. *IEEE Electr. Dev. Lett.*, 2005, **26**, 625–627.
13. Wakino, K., Minai, K. and Tamura, H., Microwave characteristics of (Zn, Sn)TiO_4 and BaO–PbO–Nd_2O_3–TiO_2 dielectric resonators. *J. Am. Ceram. Soc.*, 1974, **67**, 278–281.
14. Ohsato, H., Nishigaki, S. and Okuda, T., Superlattice and dielectric properties of BaO–R_2O_3–TiO_2 (R = La, Nd and Sm) microwave dielectric compounds. *Jpn. J. Appl. Phys.*, 1992, **31**, 3136–3138.
15. Jeong, Y. H., Kim, B. J., Jang, B. Y., Lim, J. B., Nahm, S. and Lee, H. J., MIM capacitors using $BaSm_2Ti_4O_{12}$ and $Sm_2Ti_2O_7$ dielectrics. *J. Electrochem. Soc.*, 2006, **153**(8), G755–G758.
16. Takahashi, J., Kageyama, K. and Hayashi, T., Dielectric properties of double-oxide ceramics in the system Ln_2O_3–TiO_2 (Ln = La, Nd and Sm). *Jpn. J. Appl. Phys.*, 1991, **30**, 2354–2358.
17. Laffez, P., Desgardin, G. and Raveau, B., Influence of calcinations, sintering and composition upon microwave properties of the $Ba_{6-x}Sm_{8+2x/3}Ti_{18}O_{54}$ type oxide. *J. Mater. Sci.*, 1992, **27**, 5229–5238.